metals

MDPI

Article

Electrochemical Deposition of Al-Ti Alloys from Equimolar $AlCl_3$ + NaCl Containing Electrochemically Dissolved Titanium

Vesna S. Cvetković [1,*], Nataša M. Vukićević [1], Ksenija Milićević-Neumann [2], Srećko Stopić [2], Bernd Friedrich [2] and Jovan N. Jovićević [1]

1 Department of Electrochemistry, Institute of Chemistry, Technology and Metallurgy, National Institute, University of Belgrade, Njegoševa 12, 110000 Belgrade, Serbia; vukicevic@ihtm.bg.ac.rs (N.M.V.); jovicevic@ihtm.bg.ac.rs (J.N.J.)

2 IME Process Metallurgy and Metal Recycling, RWTH Aachen University, Intzestrasse 3, 52056 Aachen, Germany; ksenija@maanaelectric.com (K.M.-N.); sstopic@metallurgie.rwth-aachen.de (S.S.); bfriedrich@metallurgie.rwth-aachen.de (B.F.)

* Correspondence: v.cvetkovic@ihtm.bg.ac.rs; Tel.: +381-11-3640-228

Received: 14 November 2019; Accepted: 31 December 2019; Published: 4 January 2020

Abstract: Al-Ti alloys were electrodeposited from equimolar chloroaluminate molten salts containing up to 0.1 M of titanium ions, which were added to the electrolyte by potentiostatic dissolution of metallic Ti. Titanium dissolution and titanium and aluminium deposition were investigated by linear sweep voltammetry and chronoamperometry at 200 and 300 °C. Working electrodes used were titanium and glassy carbon. The voltammograms on Ti obtained in the electrolyte without added Ti ions indicated titanium deposition and dissolution proceeding in three reversible steps: $Ti^{4+} \rightleftarrows Ti^{3+}$, $Ti^{3+} \rightleftarrows Ti^{2+}$ and $Ti^{2+} \rightleftarrows Ti$. The voltammograms recorded with glassy carbon in the electrolyte containing added titanium ions did not always clearly register all of the three processes. However, peak currents, which were characteristics of Al, Ti and Al-Ti alloy deposition and dissolution, were evident in voltammograms on both working electrodes used. A constant potential electrodeposition regime was used to obtain deposits on the glassy carbon working electrode. The obtained deposits were characterized by SEM, energy-dispersive spectrometry and XRD. In the deposits on the glassy carbon electrode, the analysis identified an Al and $AlTi_3$ alloy formed at 200 °C and an Al_2Ti and Al_3Ti alloy obtained at 300 °C.

Keywords: Al-Ti alloy; electrochemical co-deposition; chloroaluminate melt; XRD

1. Introduction

Intermetallic materials based on a combination of aluminium and titanium, which possess high specific strength and low weight and required stiffness and excellent oxidation resistance at elevated temperatures (particularly over 600 °C), are of increasing importance as new structural materials in aerospace industry and medicine [1–3]. Due to its ability to increase the temperature of titanium allotropic transformation, aluminum is the main alloying element for titanium. The density of aluminum is less than the density of titanium, so the addition of aluminum increases the specific strength of Ti alloys. High functional properties make the Ti-Al system the foundation of many titanium alloys. The presence of thermodynamically stable intermetallic phases in titanium-aluminum composite materials allows for and significantly enhances physical and mechanical characteristics of these systems [4].

Over the last thirty years, various processing methods have been studied to fabricate these intermetallic materials [3]. The most prominent methods for fabricating Al-Ti alloys are rapid

solidification [2], sputter deposition [5], ball milling [6], mechanical alloying [7], spark plasma sintering [8], reaction sintering of elemental powders, etc. [3].

In general, Al-Ti alloys could be electrodeposited from electrolytes containing Ti(II) species [2,3,9–11]. Electrodeposition synthesis of aluminium-titanium-based materials is a tempting process that shows the potential to replace processing methods identified earlier [2,7]. The fundamental aspects of chemistry and electrochemistry of titanium ions in molten salt electrolytes have been investigated, but data on the electrochemical behaviour of titanium ions in molten chloride/fluoride salt electrolytes are scarce and contradictory. The main barrier for successful development of an electrochemical route for aluminium-titanium alloy production is associated with the existence of different oxidation states of dissolved titanium species, namely Ti(II), Ti(III) and Ti(IV) [9,12–15].

Electrochemical deposition of aluminium-titanium intermetallics has been investigated from either an Lewis acidic chloroaluminate molten salts electrolyte made of 2:1 $AlCl_3$-NaCl or $AlCl_3$-1-ethyl-3-methylimidazolium chloride ionic liquid (IL) [1–3,7,10]. In Lewis acidic 2:1 $AlCl_3$-NaCl electrolyte systems, authors particularly studied the influence of Ti^{2+} concentration on the alloy composition and found that, with low Ti^{2+} concentrations, alloy composition depended on current density. For example, an Al_3Ti alloy containing 25% atomic fraction of titanium was deposited only at low current densities [1]. With an increase in current density, the titanium content in the alloys decreased [2]. The concentration limit of titanium in the alloy composition was proposed to be due to a mechanism, by which an Al-Ti alloy forms through the reductive decomposition of a divalent species—$Ti(AlCl_4)_2$. The electrochemical reduction of Ti^{2+} ions to metallic Ti was not observed at potentials more positive than that required for aluminium deposition, but an Al_3Ti alloy was deposited onto a copper working substrate under specific deposition conditions [2].

In comparison to other molten salt electrolytes systems, the electrochemical behaviour of titanium ions in chloride melts is different because of the stability of various oxidation states of titanium ions, which is caused by the influence of electrolyte composition [12–15] and temperature [14,15].

However, to our knowledge, there is no information published that addresses electrodeposition of Al-Ti alloys from an equimolar chloroaluminate $AlCl_3$-NaCl molten electrolyte on glassy carbon (GC) at temperatures below 300 °C. Equimolar $AlCl_3$-NaCl electrolytes have been characterised in the following ways: (a) lower vapour pressure above an equimolar melt at the same temperature applied than on an acidic $AlCl_3$-NaCl electrolyte [16,17]; (b) the aluminium deposition potential from $AlCl_4^-$ ions in an equimolar and acidic $AlCl_3$-NaCl electrolyte was more negative than the aluminium deposition potential from $Al_2Cl_7^-$ ions in an acidic melt, which provided a larger potential distance to the titanium deposition potential [18,19]; (c) the deposition current density of aluminium was greater for the reaction: $AlCl_4^- + 3e^- \rightarrow Al + 4Cl^-$, than for the reaction: $4Al_2Cl_7^- + 3e^- \rightarrow Al + 7AlCl_4^-$ for the same value of an overpotential (exceeding −60 to −80 mV) recorded with the same $AlCl_3$ concentration in the melt [1,3,18,19].

The aim of the present paper is to study titanium and aluminium co-deposition from an equimolar chloroaluminate molten salt containing Ti ions introduced by electrochemically dissolved Ti metal. This novel electrodeposition route consisting of anodic dissolution of Ti and co-deposition of Ti and Al may be a useful route for Al-Ti alloy production.

2. Materials and Methods

An equimolar mixture of $AlCl_3$ and NaCl served as a base electrolyte [20], and preparation of the electrolyte was identical to those described in previous articles [21,22].

Electrochemical measurements and electrodeposition processes were carried out at 200 and 300 °C in a three-electrode electrochemical cell. In the cell used for titanium ion introduction into the equimolar $AlCl_3$-NaCl molten salt, the working electrode (WE, an anode) was a titanium plate (Ti 99.99% Alfa Aesar, Haverhill, MA, USA), the counter electrode was titanium and the reference electrode was an aluminium rod with a diameter of 3 mm (Al 99.999% Haverhill, MA, USA). In the cells used for aluminium and titanium deposition and co-deposition, the cathode was a glassy carbon

(GC, Alfa Aesar, Haverhill, MA, USA) cylinder, a titanium plate was used as the counter electrode and the reference electrode was an aluminium rod with a diameter of 3 mm.

All the reported potentials of WEs in this work were measured relative to the equilibrium potential of the aluminium reference electrode in the melt used under given conditions.

Before the experiment, the GC WE was polished with 0.05 μm alumina powder (Merck & Co., Kenilworth, NJ, USA) and cleaned several times by sonication in ethanol and Milli-Q water with each duration of 3 min.

The aluminium electrodes were etched in solutions made of 50 vol% HF, 15 vol% H_2O, 25 vol% ammonia solution and 5 vol% H_2O_2. Thereafter, the electrodes were rinsed with deionised water and absolute ethyl alcohol and dried before use.

The Ti WEs were etched in a mixture of HF + H_2O + H_2O_2 (volume ratio: 1:20:1), rinsed with distilled water and dried before use.

Argon flow was maintained in the cell, and the electrolyte was not stirred during experiments. After the electrodes were introduced into the electrolyte, the system was left for 5 to 10 min to achieve thermal equilibrium.

The study started with recording potentiodynamic polarization curves for the Ti WE in an equimolar $AlCl_3$-NaCl melt without previously added titanium at 200 or 300 °C. The potential (measured relative to the aluminium reference electrode) was scanned from a starting value, E_I = 0.0 V, to a final value, E_F = 1.200 V, with a scan rate of 1 mV·s^{-1}.

In linear sweep voltammetry (LSV) experiments when Ti was used as a WE, and an electrolyte without previously added titanium, the potential was changed with a scan rate of 20 mV s^{-1} from a potential slightly more negative than the open-circuit potential (OCP) of Ti to a different cathodic end potential (E_C), then back to anodic potential (E_A) and finally to the starting potential. In order to examine the anodic part of the voltammograms, LSV experiments were performed, starting from the open-circuit potential to the final anodic end potential (E_A), and back to slightly more negative potential than the OCP.

Ti ions were introduced into the electrolyte by electrochemical dissolution of titanium metal with constant potentials: at 200 °C, the potential was maintained at 0.500 V; and at 300 °C, the potential was maintained at 0.450 V.

The voltammograms obtained on the GC WE in the equimolar chloroaluminate molten salts with Ti ions present started from a potential E_I, usually 0.050 V more negative than the GC OCP (measured against the aluminium reference electrode), changed to a cathodic potential limit, E_F, and back to E_I with various sweep rates.

Controlled electrodeposition onto the GC electrode in the electrolyte with previously added titanium ions was initiated 5 min. after insertion of the WE into the melt in order to allow for thermal equilibrium. Titanium and aluminium were electrodeposited at a constant overpotential at two different temperatures (200 and 300 °C). After potentiostatic deposition, the WE was taken out of the cell, washed thoroughly with absolute ethanol (Zorka-Pharma, Šabac, Serbia) in order to remove any melt residue and dried in a desiccator furnished with silica gel. The morphology and the composition of the samples deposited were explored by a scanning electron microscope (VEGA 3 model; TESCAN, Brno, the Czech Republic), equipped with an energy-dispersive spectrometer (Oxford INCA 3.2, Oxford Instruments, High Wycombe, UK) and an optical microscope (VH-Z100R model; Keyence, Osaka, Osaka Prefecture, Japan).

The deposit collected from the GC WE obtained at 200 °C was analyzed by XRD on a Philips PW1050 powder diffractometer at room temperature with Ni-filtered Cu Kα radiation (λ = 1.54178 Å) and a scintillation detector within a 2θ range of 20–85° in steps of 0.05° and a scanning time of 5 s per step, and the deposit was obtained at 300 °C by SmartLab® X-ray diffractometer (Rigaku Co., Tokyo, Japan) using Cu Kα radiation (λ = 1.542 Å). The patterns were collected within a 2θ range of 10–90° at a scan rate of 0.5°/min with a divergent slit of 0.5 mm, operated at 40 kV and 30 mA. The phases

formed during the deposition were identified by a comparison of the recorded diffraction peaks with the references from the Joint Committee on Powder Diffraction Standards (JCPDS) database.

3. Results and Discussion

3.1. Dissolution of Titanium

The composition of a solvent-fused salt has a dramatic influence on electrodeposition process of titanium [14,15]. The published works on melts used for titanium deposition (inorganic and organic melts and ILs) emphasize problems encountered with the control of electrolytes made by titanium salts dissolution. These involve titanium salt sublimation at elevated temperatures, titanium ions unwanted disproportionation and titanium oxide deposition onto electrodes including passivation. To avoid most of the mentioned problems, it was decided to introduce titanium into an equimolar $AlCl_3$-NaCl melt by electrochemically controlled dissolution. Figure 1 exhibits voltammograms obtained with a titanium electrode in an equimolar $AlCl_3$-NaCl melt at 200 °C.

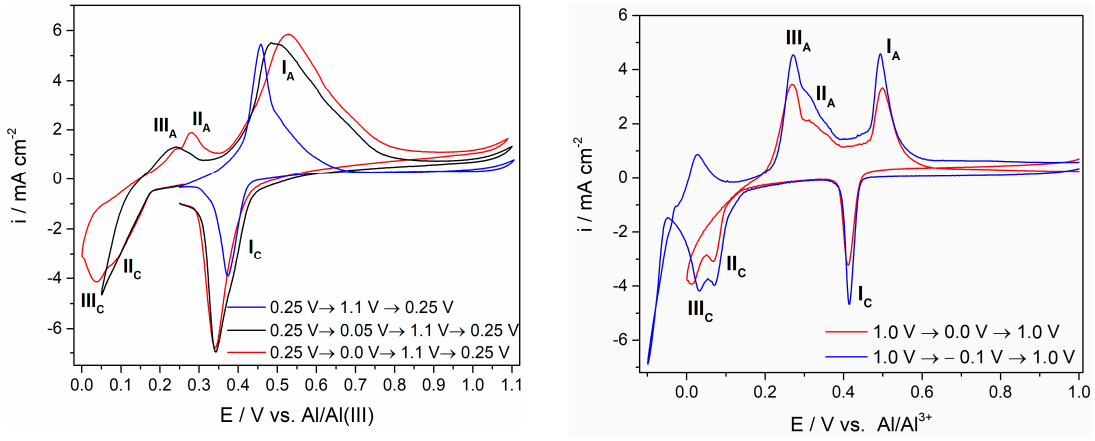

(**a**) (**b**)

Figure 1. Voltammograms with a Ti working electrode in an equimolar $AlCl_3$-NaCl melt (T = 200 °C, v = 20 mV·s^{-1}): (**a**) potential changes during the first cycle from a starting point (E_I = 0.250 V) to an anodic potential limit (E_A = 1.100 V) and then back to 0.250 V and potential changes during the second and third cycles starting from E_I = 0.250 V to different cathodic potential limits E_C, then to E_A and finally to a value E_F = 0.250 V; (**b**) potential changes during cycles from a starting point (E_I = 1.000 V) to different cathodic potential limits and back to a final value (E_F = 1.000 V).

It was found that in the presence of aluminium ions in the equimolar chloroaluminate molten salt electrolyte, the electrochemical reduction of titanium ions to metallic titanium was complicated by the formation of intermediate oxidation states of Ti^{4+}, Ti^{3+} and Ti^{2+} [1,3]. These were recorded as cathodic peaks I_C (Ti^{4+}/Ti^{3+}), II_C (Ti^{3+}/Ti^{2+}) and III_C (Ti^{2+}/Ti) and their respective anodic counterparts I_A, II_A and III_A, shown in Figure 1. These observations were similar to the results reported on Pt and Ti electrodes from an $AlCl_3$ + N-(n-butyl)pyridinium chloride (mole ratio: 2:1) melt at 25 °C [23]. The potentials related to these processes can be read from voltammograms. Their values greatly depend on temperature, the composition of electrolytes and concentrations (amounts) of dissolved titanium ions in the melt [1,3,10,13–15,24]. In the equimolar $AlCl_3$-NaCl melt used, the average recorded values of the reversible potential for the pairs Ti^{4+}/Ti^{3+}, Ti^{3+}/Ti^{2+} and Ti^{2+}/Ti were approximately 0.410, 0.190 and 0.149 V. However, they can be identified also from the potentiodynamic polarization curve of titanium recorded in the used melt at 200 °C (Figure 2). It is apparent that the potentials designated as $E_{Ti^{2+}/Ti} \approx 0.200$ V, $E_{Ti^{3+}/Ti^{2+}} \approx 0.240$ V and $E_{Ti^{4+}/Ti^{3+}} \approx 0.370$ V are in reasonably good agreement with the reversible potentials determined by the peak pairs I_C/I_A, II_C/II_A and III_C/III_A from the voltammograms in Figure 1.

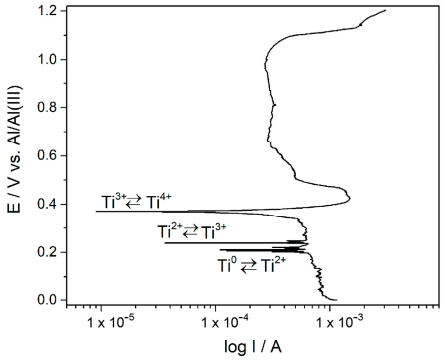

Figure 2. Potentiodynamic polarization curve of the Ti working electrode in the equimolar $AlCl_3$-NaCl melt at T = 200 °C, E_I = 0.0 V and E_F = 1.200 V.

Two important features of titanium in the equimolar $AlCl_3$-NaCl melt at 200 °C should be mentioned:

(1) The changes of the peak shape that the reaction (I_C/I_A) exhibits when recorded with different sweep rates are presented in Figure 3. It was proposed [12–15] that, in all alkali chloride melts, this pair reflects redox reaction Ti^{4+}/Ti^{3+}. Using the analysis of the relationship between the peak maximum current densities (for both cathodic and anodic currents shown in Figure 3) and the square root of a scan rate used, it was found that the relationship is linear, which confirmed that the process is a simple diffusion-controlled reversible process [25]. The positions of the other cathodic and anodic peak currents on the voltammograms (namely Ti^{3+}/Ti^{2+} and Ti^{2+}/Ti) show the reversibility of the process as well. However, they were not defined well enough in order to conduct the same analysis.

(2) The reversible potential of $Ti^{2+} \rightleftarrows Ti$ in the equimolar $AlCl_3$ -NaCl melt was recorded at ≈ 0.200 V, which is a potential positive to that required for aluminium deposition. This finding was similar to the findings observed in different electrolytes [1,3].

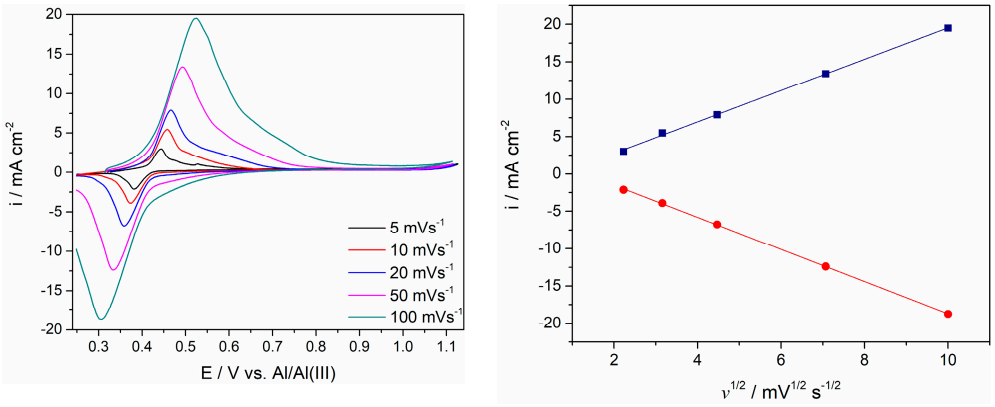

(a) (b)

Figure 3. (**a**) Voltammgrams of the Ti working electrode in the equimolar $AlCl_3$-NaCl melt at T = 200 °C with different sweep rates; (**b**) plots of anodic and cathodic peak current densities vs. square root of scan rate calculated from (**a**).

In most molten chloride/fluoride electrolytes, there are equilibria between metallic titanium and Ti^{2+}, Ti^{3+} and Ti^{4+} ions [12–15]. According to some studies in chloride electrolyte systems, metallic titanium is usually in equilibrium with two different titanium species Ti^{2+} and Ti^{3+} [9,14]. The presence of different oxidation states of titanium ions in molten chloride electrolytes and the tendency for reoxidation or disproportionation reactions mostly cause poor current efficiency and deposited product quality [9,15]. Furthermore, the melt temperature has a significant influence on equilibrium and electrodeposition processes of titanium in aforementioned electrolytes [14,15].

Taking into account the voltammograms obtained in the system used (Figure 1), the electrodissolution of titanium was done potentiostatically at 0.500 V and 200 °C and at 0.450 V and 300 °C (Figure 4). The chosen anodic potentials were sufficient enough compared to the reversible potential of the Ti^{3+}/Ti^{4+} redox couple to sustain titanium dissolution at a current density of around 1 mA·cm^{-2}. The alternate rise and drop of the dissolution current recorded in Figure 4 is due to processes of dissolution-precipitation reactions on the electrode surface at a working potential applied. Similar effects at potentials, which were anodic but close to the Ti^{2+}/Ti^{3+} reversible potential, were addressed in the literature [1,3] and were attributed to the precipitation of a Ti^{3+} product, while the breakdown of a passive film was positioned at potentials, where Ti^{4+} species generation started, i.e., at potentials close to the Ti^{3+}/Ti^{4+} reversible potential.

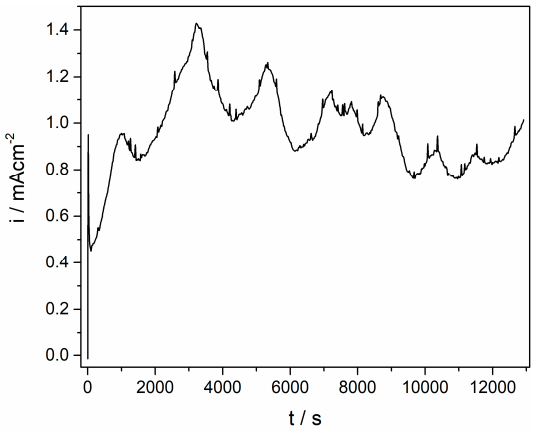

Figure 4. Anodic dissolution of the Ti working electrode at 0.500 V for 3.6 h in the equimolar $AlCl_3$–NaCl melt at T = 200 °C.

Thus, a melt that was equimolar in $AlCl_3$ and NaCl and contained ≈ 0.1 M titanium was prepared to be used in experiments involving titanium and aluminium electrodeposition on GC. The Ti molarity was calculated from the Ti anode mass lost during controlled potentiostatic dissolution (Faraday's law applied to Ti → Ti^{2+}) and from the slopes in Figure 3, following the procedure proposed in a similar system using Randles-Sevcik equation [3,26]:

$$i_p = 0.4463\left(\frac{F^3}{RT}\right)^{\frac{1}{2}} n^{\frac{3}{2}} A D_0^{\frac{1}{2}} C_0^* v^{\frac{1}{2}}, \quad (1)$$

where i_p is the peak current in amperes; v is the sweep rate in V·s^{-1}; C_0^* is the concentration in mol·cm^{-3}, D_0 is the diffusion coefficient in cm^2·s^{-1}; A is the area of an electrode in cm^2, n is the number of electrons, F is the Faraday's constant; R is the gas constant; T is the temperature. Both methods showed that the concentration of titanium in the melt used was around 0.1 M. A titanium anode was used to replace (by its dissolution) Ti ions reduced to titanium metal from the electrolyte. Thus, the Ti ions concentration was kept close to a wanted value during experiments.

3.2. Deposition of Titanium and Aluminium onto GC

The LSV results of the GC WE in the equimolar $AlCl_3$-NaCl melt used with anodically dissolved titanium and recorded at 200 and 300 °C are presented in Figures 5 and 6. The obtained voltammograms were very similar to those obtained on W, Cu, mild steel and Pt in chloride and fluoride/chloride inorganic melts and ILs with different titanium concentrations and working temperatures [1,3,10,15,23].

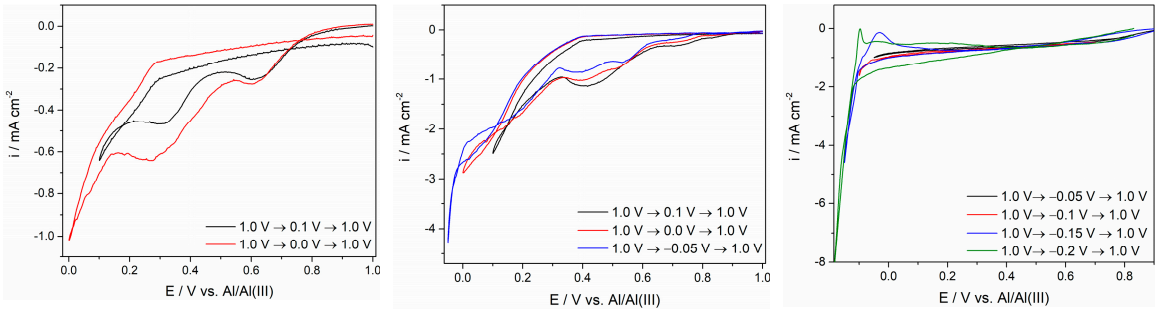

(a) (b) (c)

Figure 5. Voltammograms of the glassy carbon (GC) working electrode in the equimolar $AlCl_3$-NaCl melt containing anodically dissolved Ti, obtained at different cathodic potential limits and at T = 200 °C with different sweep rates: (**a**) ν = 5 mV·s^{-1}; (**b**) ν = 20 mV·s^{-1}; (**c**) ν = 5 mV·s^{-1}.

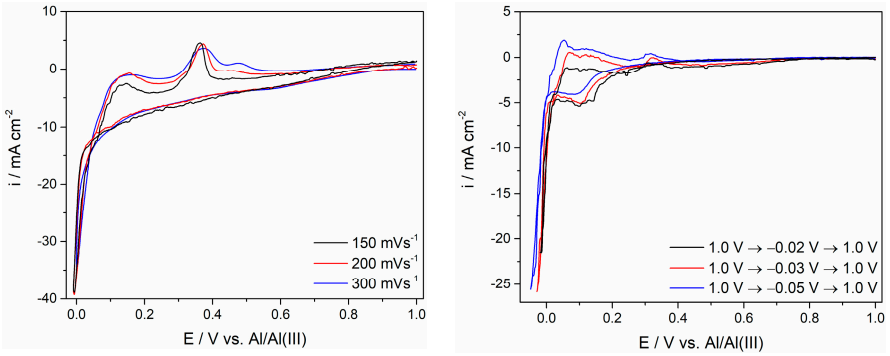

(a) (b)

Figure 6. Voltammograms obtained on the GC working electrode in the equimolar $AlCl_3$-NaCl melt containing anodically dissolved Ti at T = 300 °C on different conditions: (**a**) potential change: E_I = 1.000 V to E_F = 0.0 V with different sweep rates; (**b**) at different cathodic potential limits at a constant sweep rate ν of 50 mV·s^{-1}.

The voltammograms in Figures 5 and 6 do not exhibit well-defined cathodic and anodic sides of the voltammograms, as was the case with the titanium WE in the same electrolyte with a much lower titanium concentration (Figure 1). At a lower temperature (Figure 5), the cathodic side of the voltammogram was better defined than its anodic counterpart and tentatively suggests three current increases reflecting all three steps of Ti^{4+} ions being reduced to Ti metal at potentials more positive than the aluminium reversible potential. It appears that the peak potentials, although not always easily identified, approached the values recorded for the same reactions on the Ti WE (see Figure 1). At a higher temperature, the peak current density structures were recognizable for both the cathodic and anodic sides of the voltammograms. However, the anodic side of the voltammograms was better defined, showing all three expected oxidation peaks after the applied cathodic potential limit was made more negative than −0.020 V.

When the cathodic potential limit was pushed further to an aluminium overpotential region, pronounced cathodic currents were recorded in the electrolyte with 0.1 M of titanium ions, independent of the temperature applied. The anodic response to the entrance into the aluminium overpotential region showed peaks, suggesting dissolution of Ti and Al and most probably dissolution of an Al-Ti alloy. The charge under the curve of the corresponding anodic peaks, however, did not always equal those under the curves of the cathodic counterparts.

The data obtained by LSV were used to define the potentials needed for the electrodeposition of an Al-Ti alloy, which was the primary goal of this work. The chronoamperometic response in the form of i = f(t) to an overpotential of −0.085 V applied to the GC WE for two hours at 200 °C in the equimolar

$AlCl_3$-NaCl melt containing 0.1 M of titanium ions is presented in Figure 7a. When the falling part of the transient in Figure 7a was transformed into the form of $i = f(t^{-1/2})$, a linear relationship became obvious [25], shown in Figure 7b, suggesting that after approximately 400 s, the Al and Ti deposition was proceeded under diffusion control. With all other conditions being the same, the chronopotentiograms recorded at 300 °C on the GC electrode were very similar in shape, with deposition current densities being about two times greater than the same potential applied at 200 °C.

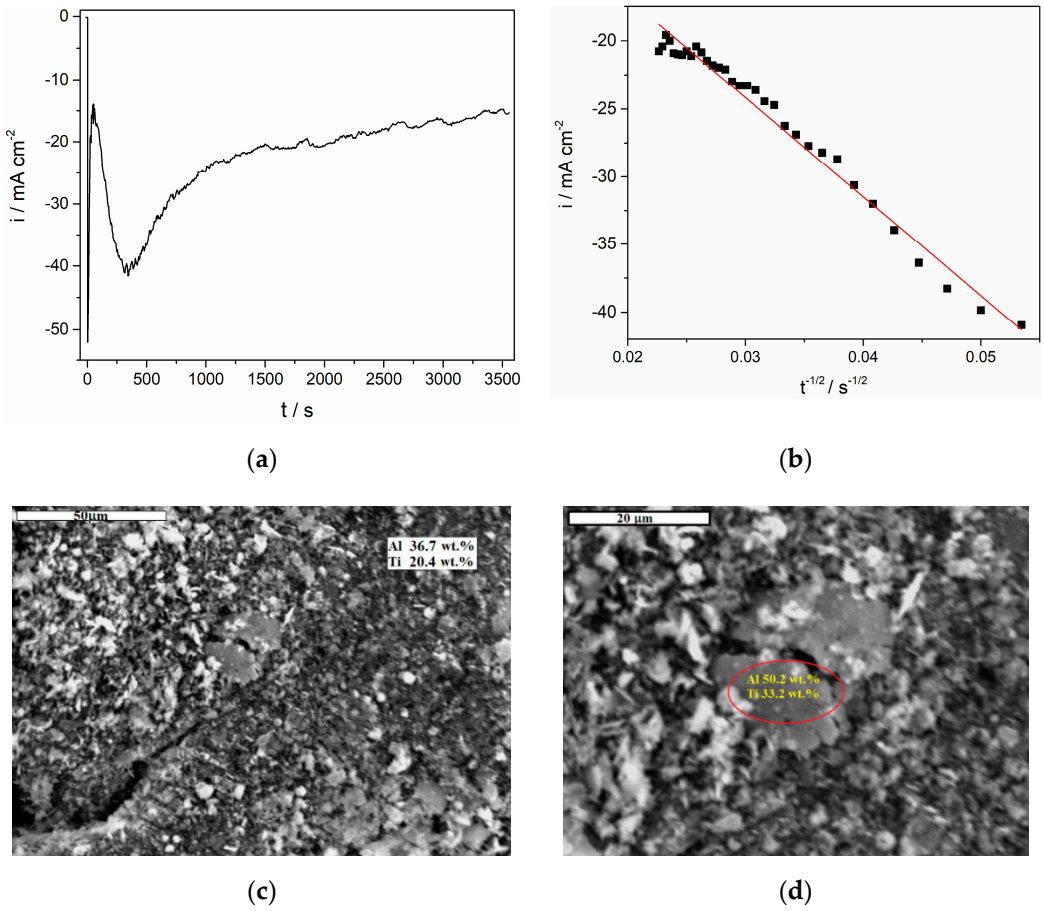

Figure 7. Potentiostatic deposition on the GC working electrode from the equimolar $AlCl_3$-NaCl melt containing anodically dissolved Ti at −0.085 V and 200 °C for two hours: (**a**) current–time transient of the deposition; (**b**) current as a function of $t^{-1/2}$ for the falling part of the transient in (a); (**c**,**d**) SEM photographs of the deposit obtained with energy-dispersive spectroscopy (EDS) results embedded.

For both temperatures applied, thick but nonuniform deposits were obtained (Figure 7c,d and Figure 8). At a higher magnification, grains of different sizes similar to those obtained from $AlCl_3$-BMIC ILs on mild steel published recently [27] can be observed. The energy-dispersive spectroscopy (EDS) analysis made from a larger portion of the same deposits (approximately 400 µm^2) reported 36.7 wt. % of Al and 20.4 wt. % of Ti (Figure 7c). In Figure 7d, a result of EDS analysis for one of the larger grains in the deposit is presented numerically (in the inserted circle), and it suggests presence of 50.2 wt. % of Al and 33.2 wt. % of Ti. The deposits obtained at 300 °C and −0.020 V after two hours showed a larger average grain size than the deposit obtained after two hours at −0.085 V and 200 °C (Figure 8).

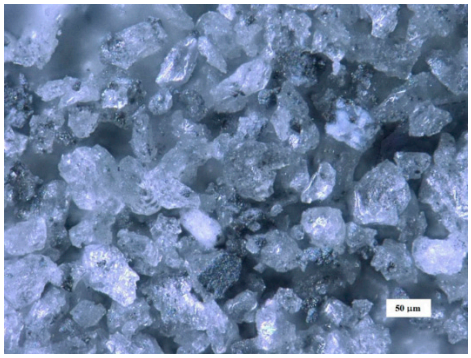

Figure 8. Optical microscopy image of the deposit obtained on the GC electrode from the equimolar $AlCl_3$-NaCl melt containing anodically dissolved Ti at −0.020 V and 300 °C for two hours.

Data acquired from the XRD analysis of the deposits are shown in Figure 9.

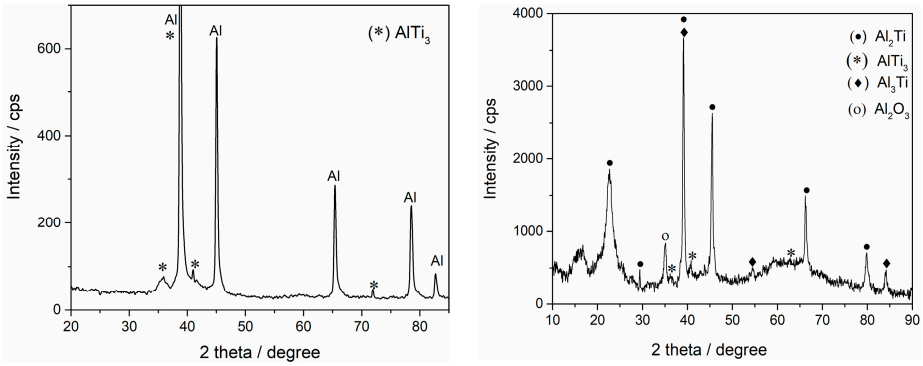

(**a**) (**b**)

Figure 9. XRD patterns of the deposits obtained potentiostatically on the GC electrode on different conditions: (**a**) at −0.085 V and 200 °C for two hours; (**b**) at −0.020 V and 300 °C for two hours.

The analysis for the deposit obtained at 200 °C (Figure 9a) exhibited diffraction peaks at 2θ = 35.9° with reflection (200), 38.95° with reflection (002), 41.036° with reflection (201) and 71.97° with reflection (203), which are characteristics of a hexagonal $AlTi_3$ alloy (JCPDS No. 03-065-7534). Several stronger diffraction peaks at 2θ = 38.47°, 44.73°, 65.13°, 78.22° and 82.43° with the respective reflections (111), (200), (220), (311) and (222) should be attributed to face-centered cubic Al (JCPDS No. 00-004-0787). The spectrum indicates no evidence of additional peaks, implying that the deposit produced by the electrochemical deposition method in this study was relatively pure.

According to the data from XRD analysis of the deposit obtained on GC at a higher temperature (300 °C), dominating alloy appeared to be Al_2Ti (Figure 9b). The spectrum gives diffraction peaks at 2θ = 22.68°, 29.37°, 38.99°, 45.66°, 66.55° and 79.94°, with the respective reflections (101), (008), (116), (200), (220) and (316), which are characteristics of body-centered tetragonal Al_2Ti (JCPDS No. 00-052-0861). Peaks in the spectrum at 2θ = 39.15°, 54.32° and 84.15° with the respective reflections (112), (211) and (224) can be attributed to body-centered tetragonal Al_3Ti (JCPDS No.03-065-2667). The spectrum also indicates characteristics of a hexagonal $AlTi_3$ alloy, of which the peaks are at 2θ = 35.76°, 40.84° and 62.69° with the respective reflections (200), (201) and (103) (JCPDS No. 03-0-052-0859). The peak at 2θ = 35.15° can be associated with the trace of Al_2O_3 (JCPDS No: 00-046-1212), implying that it was not possible to handle a sample without exposing it to the atmosphere.

Each of the peaks attributed to a certain alloy were chosen from a group of five or seven highest peak intensities as defined by the JCPDS database for the mentioned alloy. However, due to the fact that the Al-Ti binary phase diagram is not fully understood [4,28,29] and the fact that we only presented

initial experimental results, there is a space for improvement in attribution of the peak positions in XRD analysis of the obtained electrodeposits in the future.

The $AlTi_3$ alloy obtained on the GC WE from the equimolar $AlCl_3$-NaCl melt with titanium ions added by electrodissolution of metal Ti is a finding different from a $TiAl_3$ alloy predominantly produced electrochemically on Cu and mild steel from electrolytes reported in the literature [1,2,7,10,11]. The $AlTi_3$ alloy is hexagonal in structure, and in the Al-Ti phase diagram, it appears in the composition region of 13–25 wt. % Al (i.e., 75–87 wt. % Ti) at temperatures below 1200 °C [30]. The $AlTi_3$ intermetallic compound is largely accepted as having a variable composition, with a wide homogeneity domain and as an intermetallic compound formed by order-disorder transformation (α_{Ti}) ↔ ($AlTi_3$). This aluminide is emerging as a revolutionary material for high-temperature applications and aeronautical industry [31, 32].

Al_3Ti is an intermediate phase of a tetragonal structure and appears in the binary phase diagram in a composition region, where the Al mass is between 75% and 100% [28]. The Al_3Ti alloy has a great potential application in aerospace and automobile as a high-temperature structural material, but it has poorest ductility among three typical Al-Ti alloys ($AlTi_3$, AlTi and Al_3Ti), which limits its engineering applications [33].

The Al_2Ti compound is considered stable up to 1216 °C, existing with a very narrow Al range between 60 and 67 at % [29]. Al_2Ti is one of the four intermetallic phases in the Ti-Al binary system that are stable below 1150 °C [34]. Al_2Ti is a very promising material for elevated-temperature applications.

However, although the Al-Ti binary phase diagram has been intensively studied, it still cannot be considered fully reliable [4,28,29]. It seems that there are 12 intermetallic compounds recognised [35]. According to the Ti-Al phase diagram, there can be up to seven stable intermetallic phases. The most stable intermetallic phases that increase the physico-mechanical properties of titanium aluminide are γ-TiAl, α2-Ti_3Al and γ-TiAl + α2-Ti_3Al. Lately, it was pointed out that $AlTi_3$ and AlTi intermetallic compounds are largely accepted as having variable compositions, with a wide homogeneity domain, while Al_2Ti and Al_5Ti_2 are accepted as having constant compositions [29]. According to the same authors, Al_3Ti is treated as an intermetallic compound with a variable composition or with a constant composition [29]. If thermal procedures are used, all of the abovementioned intermetallics can be produced at temperatures above 1110 °C.

When electrochemical co-deposition is used as a procedure for binary Al-Ti alloy generation, such high temperatures are not required. The mechanism of alloy formation in this case includes nanoscale relationships between adatoms of co-depositing metals on the substrate, such as interdiffusion in a solid state [18,36]. Interdiffusion phenomena were investigated in the Ti-Al system (a Ti region from 25 to 100 at %), but only at elevated temperatures (between 516 and 1200 °C). In a temperature range between 516 and 642 °C, metallic Ti, as well as Ti-Al alloys, was coated with a solid layer of metallic Al, and interdiffusion was studied. A well-adhered layer of $TiAl_3$ was formed, while no other intermetallic compounds were observed and no solid solution of Al in Ti was recorded [37]. In another study, interdiffusion phenomena were investigated in a Ti-Al system but at higher temperatures (between 768 and 972 °C) [38]. In the Al-rich part of the diagram, the Ti_2Al_5 phase was identified. It was found that, at temperatures between 768 and 865 °C, Ti was the more mobile element in the Ti_3Al phase whereas in the Al-richer compounds Al was the more mobile element at temperatures between 784 and 972 °C. The results of the studies in our work indicated appreciable interdiffusion between the co-deposited Al and Ti even at 200 and 300 °C, which led to the formation of Al_3Ti, Al_2Ti and $AlTi_3$.

4. Conclusions

The electrodeposition of Al-Ti alloys from an equimolar $AlCl_3$-NaCl melt on a GC electrode was successfully performed. It was shown that there is a novel way to obtain Al-Ti alloys, such as $AlTi_3$, Al_2Ti and Al_3Ti, in a very controlled manner under favorable and technologically suitable conditions.

The voltammograms generated from a system of a Ti WE in the equimolar $AlCl_3$-NaCl melt at 200 and 300 °C without introducing Ti ions indicated titanium deposition and dissolution proceeding in

three reversible steps: $Ti^{4+} \rightleftarrows Ti^{3+}$, $Ti^{3+} \rightleftarrows Ti^{2+}$ and $Ti^{2+} \rightleftarrows Ti$, occurring at potentials more positive than the reversible potential of Al. The reversible potential of titanium in the equimolar $AlCl_3$-NaCl melt was identified as ≈ 0.200 V, and the starting deposition potential of titanium onto Ti was ≈ 0.020 V at 200 and 300 °C.

The titanium deposition starting potential on the GC electrode in the electrolyte made of an equimolar $AlCl_3$-NaCl melt containing ≈ 0.1 M of titanium ions appeared to be between 0.050 and 0.0 V for both temperatures applied (200 and 300 °C). However, we did not succeed in depositing pure titanium without aluminium, because their deposition potentials were very close.

The XRD analysis of the deposits revealed that $AlTi_3$, Al_2Ti and Al_3Ti alloys were generated on the GC electrode, with $AlTi_3$ dominating at a lower temperature and Al_2Ti dominating at a higher temperature.

The results obtained in this work suggest new possibilities of aluminium-titanium alloys formation (including $AlTi_3$) using low temperatures via a better controlled process.

Author Contributions: V.S.C. designed and managed the research and participated in the manuscript preparation; N.M.V. performed most of the experiments and participated in the manuscript preparation; K.M.-N., S.S. and B.F. helped with the corrections of the manuscript; J.N.J. supervised the experiments and the manuscript writing. S.S. and B.F. from RWTH Aachen University provided funding for publication. All authors discussed the results and commented on the manuscript. All authors have read and agreed to the published version of the manuscript.

Funding: Part of the research was supported by the funds of the bilateral research project (ID: 451-03-01971/2018-09/4) supported by the Ministry of Education, Science and Technological Development of the Republic of Serbia and German Academic Exchange Service (DAAD).

Acknowledgments: Vesna S. Cvetković and Nataša M. Vukićević acknowledge the financial support for the investigation received from the Ministry of Education, Science and Technological Development of the Republic of Serbia.

Conflicts of Interest: The authors declare no conflicts of interest.

References

1. Stafford, G.R. The Electrodeposition of Al_3Ti from Chloroaluminate Electrolytes. *J. Electrochem. Soc.* **1994**, *141*, 945–953. [CrossRef]
2. Tsuda, T.; Hussey, C.L.; Stafford, G.R.; Bonevich, J.E. Electrochemistry of titanium and the electrodeposition of Al-Ti alloys in the Lewis acidic aluminum chloride-1-ethyl-3-methylimidazolium chloride melt. *J. Electrochem. Soc.* **2003**, *150*, C234–C243. [CrossRef]
3. Stafford, G.R.; Moffort, T.P. Electrochemistry of Titanium in Molten $2AICI_3$-NaCI. *J. Electrochem. Soc.* **1995**, *142*, 3288–3296. [CrossRef]
4. Kosova, N.; Sachkov, V.; Kurzina, I.; Pichugina, A.; Vladimirov, A.; Kazantseva, L.; Sachkova, A. The preparation of the Ti-Al alloys based on intermetallic phases. *IOP Conf. Ser. Mater. Sci. Eng* **2016**, *112*, 012039. [CrossRef]
5. Yan, Q.; Yoshioka, H.; Habazaki, H.; Kawashima, A.; Asami, K.; Hashimoto, K. Passivity and its breakdown on sputter-deposited amorphous AlTi alloys in a neutral aqueous solution with Cl^-. *Corros. Sci.* **1990**, *31*, 401–406. [CrossRef]
6. Moon, K., II; Lee, K.S. Study of the microstructure of nanocrystalline Al-Ti alloys synthesized by ball milling in a hydrogen atmosphere and hot extrusion. *J. Alloys Compd.* **1999**, *291*, 312–321. [CrossRef]
7. Stafford, G.R.; Tsuda, T.; Hussey, C.L. Order/disorder in electrodeposited aluminum-titanium alloys. *J. Min. Metall.* **2003**, *39*, 23–42. [CrossRef]
8. Yang, Y.F.; Qian, M. Spark plasma sintering and hot pressing of titanium and titanium alloys. In *Titanium Powder Metallurgy: Science, Technology and Application*; Elsevier Inc.: Amsterdam, The Netherlands, 2015; pp. 219–236. [CrossRef]
9. Haarberg, G.M.; Kjos, O.S.; Martinez, A.M.; Osen, K.S.; Skybakmoen, E.; Dring, K. Electrochemical behaviour of dissolved titanium species in molten salts. *ECS Trans.* **2010**, *33*, 167–173. [CrossRef]
10. Tsuda, T.; Hussey, C.L.; Stafford, G.R. Electrodeposition of Titanium-aluminum alloys in the lewis acidic aluminum chloride-1-ethyl-3-methylimidazolium chloride molten salt. *ECS Proc. Vol.* **2002**, *2002*, 650–659. [CrossRef]

11. Uchida, J.; Seto, H.; Shibuya, A. Electrodeposition of Al-Ti alloy from chloroaluminate bath. *J. Surf. Finish. Soc. Jpn.* **1995**, *46*, 1167–1172. [CrossRef]
12. Uda, T.; Okabe, T.H.; Waseda, Y.; Awakura, Y. Electroplating of titanium on iron by galvanic contact deposition in NaCl-$TiCl_2$ molten salt. *Sci. Technol. Adv. Mater.* **2006**, *7*, 490–495. [CrossRef]
13. Zhu, X.; Wang, Q.; Song, J.; Hou, J.; Jiao, S.; Zhu, H. The equilibrium between metallic titanium and titanium ions in LiCl–KCl melts. *J. Alloys Compd.* **2014**, *587*, 349–353. [CrossRef]
14. Song, J.; Wang, Q.; Wu, J.; Jiao, S.; Zhu, H. The influence of fluoride ions on the equilibrium between titanium ions and titanium metal in fused alkali chloride melts. *Faraday Discuss.* **2016**, *190*, 421–432. [CrossRef] [PubMed]
15. Song, J.; Xiao, J.; Zhu, H. Electrochemical behavior of titanium ions in various molten alkali chlorides. *J. Electrochem. Soc.* **2017**, *164*, E321–E325. [CrossRef]
16. Trémillon, B.; Letisse, G. Proprietes en solution dans le tetrachloroaluminate de sodium fondu I. systemes "acide-base". *J. Electroanal. Chem. Interfacial Electrochem.* **1968**, *17*, 371–386. [CrossRef]
17. Del Duca, B.S. Electrochemical behavior of the aluminum electrode in molten salt electrolytes. *J. Electrochem. Soc.* **1971**, *118*, 405–411. [CrossRef]
18. Stafford, G.R.; Hussey, C.L. Electrodeposition of Transition Metal-Aluminum Alloys from Chloroaluminate Molten Salts. In *Advances in Electrochemical Science and Engineering*; Alkire, R.C., Kolb, D.M., Eds.; Wiley-VCH Verlag GmbH: Winheim, Germany, 2001; Volume 7, pp. 275–348.
19. Kan, H.M.; Wang, Z.W.; Wang, X.Y.; Zhang, N. Electrochemical deposition of aluminum on W electrode from $AlCl_3$-NaCl melts. *Trans. Nonferrous Met. Soc. China* **2010**, *20*, 158–164. [CrossRef]
20. Berg, W.R.; Hjuler, A.H.; Bjerrum, N. Phase diagram of the NaCl-$AlCl_3$ system near equimolar composition, with determination of the cryoscopic constant, the enthalpy of melting and oxid contaimination. *Inorg. Chem.* **1984**, *23*, 557–565. [CrossRef]
21. Radović, B.S.; Cvetković, V.S.; Edwards, R.A.H.; Jovićević, J.N. Al–Fe alloy formation by aluminium underpotential deposition from $AlCl_3$+NaCl melts on iron substrate. *Int. J. Mater. Res.* **2011**, *102*, 59–68. [CrossRef]
22. Vukićević, N.M.; Cvetković, V.S.; Jovanović, L.; Stevanović, S.I.; Jovićević, J.N. Alloy Formation by Electrodeposition of Niobium and Aluminium on Gold from Chloroaluminate Melts. *Int. J. Electrochem. Sci.* **2017**, *12*, 1075–1093. [CrossRef]
23. Ali, M.R.; Nishikata, A.; Tsuru, T. Electrodeposition of Al-Ti alloys from aluminum chloride-N-(n-butyl)pyridinium chloride room temperature molten salt. *Indian J. Chem. Technol.* **2003**, *10*, 14–20.
24. Endres, F.; Zein El Abedin, S.; Saad, A.Y.; Moustafa, E.M.; Borissenko, N.; Price, W.E.; Wallace, G.G.; MacFarlane, D.R.; Newman, P.J.; Bund, A. On the electrodeposition of titanium in ionic liquids. *Phys. Chem. Chem. Phys.* **2008**, *10*, 2189–2199. [CrossRef] [PubMed]
25. Greef, R.; Peat, R.; Peter, L.M.; Pletcher, D.; Robinson, J. *Instrumental Methods in Electrochemistry*, 1st ed.; Kemp, T.J., Ed.; Ellis Horwood Limited: Chichester, UK, 1985.
26. Bard, A.J.; Faulkner, L.R. *Electrochemical Methods. Fundamentals and Applications*, 2nd ed.; Jonh Wiley & Sons, Inc.: New York, NY, USA, 2001.
27. Xu, C.; Hua, Y.; Zhang, Q.; Li, J.; Lei, Z.; Lu, D. Electrodeposition of Al-Ti alloy on mild steel from $AlCl_3$ -BMIC ionic liquid. *J. Solid State Electrochem.* **2017**, *21*, 1349–1356. [CrossRef]
28. Landolt, H.; Börnstein, R. *Phase Equilibria, Crystallographic and Thermodynamic Data of Binary Alloys*; Springer: Berlin/Heidelberg, Germany, 1991. [CrossRef]
29. Batalu, D.; Coşmeleaţă, G.; Aloman, A. Critical analysis of the Ti-Al phase diagrams. *UPB Sci. Bull. Ser. B Chem. Mater. Sci.* **2006**, *68*, 77–90.
30. Massalski, T.B.; Okamoto, H.; Subramanian, P.R.; Kacprzak, L. *Binary Alloy. Phase Diagrams*, 2nd ed.; Massalski, T., Okamoto, H., Subramanian, P.R., Kacprzak, L., Eds.; ASM International, Materials Park: Geauga County, OH, USA, 1990; Volume 1–3.
31. Djanarthany, S.; Viala, J.C.; Bouix, J. An overview of intermetallic matrix composites based on Ti_3Al and TiAl. *Mater. Chem. Phys.* **2001**, *72*, 301–319. [CrossRef]
32. Froes, F.H.; Suryanarayana, C.; Eliezer, D. Synthesis, properties and applications of titanium aluminides. *J. Mater. Sci.* **1992**, *27*, 5113–5140. [CrossRef]

33. Wei, N.; Han, X.; Zhang, X.; Cao, Y.; Guo, C.; Lu, Z.; Jiang, F. Characterization and properties of intermetallic Al_3Ti alloy synthesized by reactive foil sintering in vacuum. *J. Mater. Res.* **2016**, *31*, 2706–2713. [CrossRef]
34. Benci, J.E.; Ma, J.C.; Feist, T.P. Evaluation of the intermetallic compound Al_2Ti for elevated-temperature applications. *Mater. Sci. Eng. A* **1995**, *192–193*, 38–44. [CrossRef]
35. Villars, P.; Calvert, L. *Pearson's Handbook of Crystallographic Data for Intermetallic Phases*, 2nd ed.; Villars, P., Calvert, L., Eds.; ASM International, Materials Park: Geauga, OH, USA, 1991.
36. Cvetković, V.S.; Vukićević, N.M.; Jovićević, J.N. Aluminium and Magnesium Alloy Synthesis by Means of Underpotential Deposition from Low Temperature Melts. In *Metals and Metal-Based Electrocatalytic Materials for Alternative Energy Sources and Electronics*; Stevanović, J., Ed.; Nova Science Publisher: New York, NY, USA, 2019; pp. 371–423.
37. Van Loo, F.J.J.; Rieck, G.D. Diffusion in the titanium-aluminium system-I. Interdiffusion between solid Al and Ti or Ti-Al alloys. *Acta Metall.* **1973**, *21*, 61–71. [CrossRef]
38. Van Loo, F.J.J.; Rieck, G.D. Diffusion in the titanium-aluminium system-II. Interdiffusion in the composition range between 25 and 100 at.% Ti. *Acta Metall.* **1973**, *21*, 73–84. [CrossRef]